

Water exchange  
Dardanelles Strait  
Hydraulic control  
Two-layer model  
Entrainment  
Échange d'eau  
Détroit des Dardanelles  
Contrôle hydraulique  
Modèle à deux couches  
Entraînement

# A two-layer model of water exchange through the Dardanelles Strait

Temel OĞUZ, H. Ibrahim SUR

Institute of Marine Sciences, Middle East Technical University, P.O. Box 28, Erdemli-İçel, Turkey.

Received 15/4/88, in revised form 29/8/88, accepted 6/9/88.

## ABSTRACT

Water exchange through the Dardanelles Strait is studied by a two-layer model which considers the laterally averaged flow formed by two homogeneous layers of differing density separated by an entraining interface. The model response is discussed in terms of observations from the strait. In particular, the observed asymmetry and rapid transition at the interface depth as well as the intense mixing which occurs in the southwestern reaches of the strait are found to be related to the hydraulic characteristics of the flow. It appears that the Dardanelles exercises efficient hydraulic controls on the upper-layer flow, due to contraction at Nara Pass and abrupt expansion of the width at its Aegean exit. Supercritical regions of the upper-layer flow downstream of the control sections are identified as being the regions of increased currents, shallower surface layer depth and intense net interfacial transport of lower-layer water into the upper layer. Sensitivity studies show that the value of the interfacial friction coefficient is an important parameter influencing the structure of the water exchange along the strait.

*Oceanol. Acta*, 1989, 12, 1, 23-31.

## RÉSUMÉ

Un modèle à deux couches de l'échange d'eau à travers le détroit des Dardanelles

L'échange d'eau à travers le détroit des Dardanelles a été étudié par un modèle à deux couches, qui considère le flux moyen latéral formé par deux couches homogènes de densités différentes, séparées par une interface d'entraînement. La réponse du modèle est discutée en fonction des observations sur le détroit. En particulier, on montre que l'asymétrie observée et la transition rapide à la profondeur de l'interface, ainsi que le mélange intense dans le sud-ouest du détroit, sont liées aux caractéristiques hydrauliques du flux. Il apparaît que le détroit des Dardanelles exerce des contrôles hydrauliques efficaces sur l'écoulement de la couche supérieure, par le resserrement du passage de Nara et son brusque élargissement à sa sortie de l'Égée. Les régions supercritiques de l'écoulement superficiel vers l'aval des sections de contrôle sont identifiées comme les régions de courants forts. L'épaisseur de la couche superficielle est moindre, et le transport à travers l'interface de l'eau de la couche inférieure vers la couche supérieure est net et intense. Les vents du Nord-Est qui soufflent dans la direction de l'écoulement de la couche supérieure, provoquent une accélération des courants et l'intensification de l'entraînement du flux net vers le haut. Les études de sensibilité montrent que la valeur du coefficient de frottement à l'interface est un paramètre important qui influence la structure de l'échange d'eau le long de détroit.

*Oceanol. Acta*, 1989, 12, 1, 23-31.

## INTRODUCTION

The Dardanelles Strait constitutes the southeasternmost component of the Turkish Strait System (hereafter referred to as TSS) and is a pathway between the

Aegean basin of the Mediterranean Sea and the Marmara Sea, which further communicates with the Black Sea through the Bosphorus Strait at its other extremity (Fig. 1 a, b). It has an approximate length of 65 km, and an average width and depth of 3.5 km and 55 m

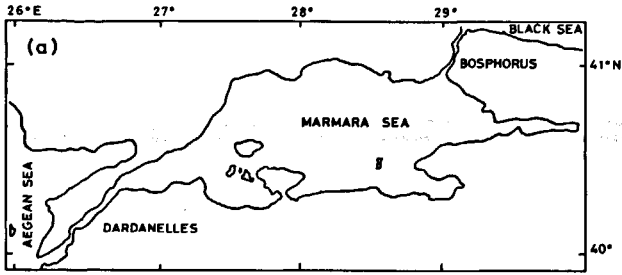


Figure 1

Location map of the Turkish Strait System: a) in relation to the Aegean and Black Seas; and b) the Dardanelles including also the locations of the hydrographic stations.

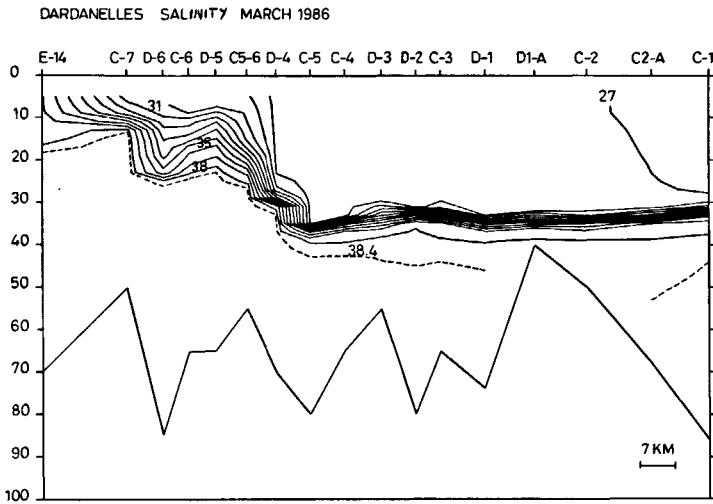
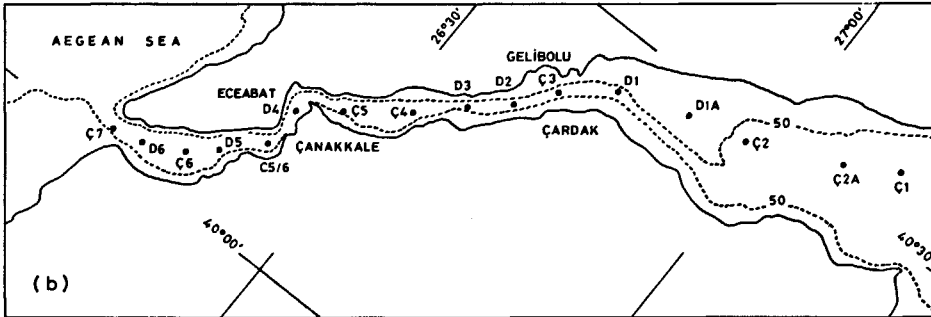


Figure 2  
Salinity transects in the Dardanelles during March 1986.

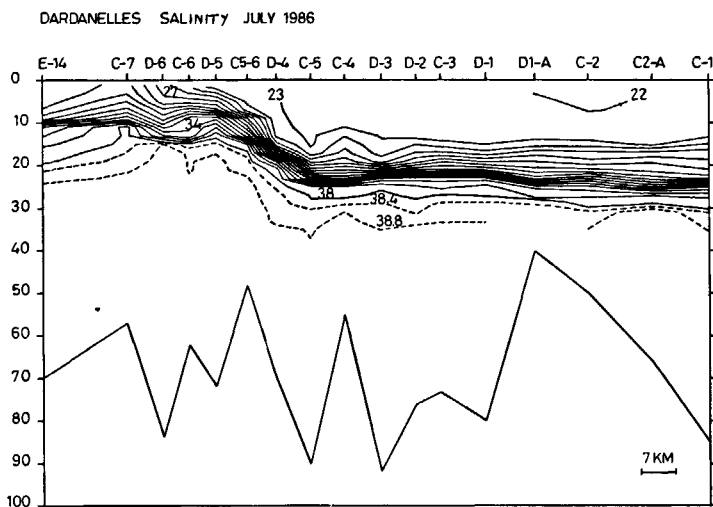


Figure 3  
Salinity transects in the Dardanelles during July 1986.

respectively. Whereas the strait is connected to the Western Marmara basin by a gradually widening junction region, it is terminated at the Aegean Sea by an abrupt opening. As far as its flow dynamics are concerned, its most distinguishing geometrical feature is the channel constriction found immediately southwest of the sharp bending region. The narrowest section, the so-called Nara Pass, where the width diminishes to 1.2 km, evidently plays an important role in the dynamical characteristics of the flow.

A detailed description of the oceanographic characteristics of the Dardanelles Strait and the TSS in general is given by Özsoy *et al.*, (1986). As an integral part of the TSS, the Dardanelles reflects a persistent two-layer flow structure associated with the two-layer stratification. The density profile is dominated by salinity alone, even though significant seasonal variations take place in temperature. Generally speaking, the upper levels consist of brackish water of Black Sea origin flowing towards the Aegean Sea, the bottom layer being characterized by saltier Mediterranean water traversing the strait in a northeasterly direction. The largest flow towards the Aegean occurs in the late spring and summer, corresponding to the periods at which the precipitation and river runoff discharged into the Black Sea increase substantially.

Mixing of lower-layer waters into the upper layer is one of the characteristic features of the Dardanelles that deserves special attention. As shown by two typical salinity transects in Figures 2 and 3, the northeastern part of the strait, constituting the region between stations D1 and C5, is characterized by a relatively sharp interfacial zone across which negligible mixing takes place between the layers. Immediately after station D4, the upper-layer salinities become much less uniform, implying that the bulk of the mixing occurs essentially within the lower half of the Dardanelles. Vertical mixing is triggered by the sharp bending section located between stations C5 and D4, and is intensified after the upper-layer flow passes through the Nara contraction. Consequently, almost 4-5 ppt changes occur in the

upper-layer salinities between the two extremities of the Dardanelles. Utilizing the long-term average values of salinity and flow rate, the two-layer water and salt budget analyses of the entire TSS have shown that some 20% of the Aegean influx is entrained by the surface water and returns as an upper-layer flow before reaching the Marmara Sea (Özsoy *et al.*, 1986).

Depending on the particular density and flow conditions in the adjoining basins, it is known that certain geometrical features such as sills, contractions and sudden widenings may act as controls on the flow, which may then pass through the critical state (Armi, 1986; Armi, Farmer, 1986; Farmer, Armi, 1986; Stacey, Zedel, 1986; Wang, 1987). Examples of flows subjected to hydraulic controls have been given by Stigebrandt (1981), Armi and Farmer (1985) and Farmer and Denton (1985). The locations of intense mixing, observed asymmetry and rapid transition of the interface depth displayed in Figures 2 and 3, as well as those reported in Özsoy *et al.* (1986), seem to indicate that the Dardanelles may also exercise similar hydraulic controls on the flow due to the contraction at the Nara Pass and the abrupt widening at the Aegean exit sections.

In the present paper we examine the dynamics of the two-layer flow in the Dardanelles Strait, with particular attention to the possible existence of hydraulic controls, the locations of the latter and the manner in which they affect the mixing characteristics and the two-way exchange through the strait. A two-layer numerical model is applied to the laterally averaged flow in which two homogeneous layers of differing density are separated by an interface allowing for entrainment between the layers. We assume that the longitudinal density variations do not alter the main features of the flow appreciably, so that each layer has a horizontally uniform density structure. We consider these simplifications to make the analysis more convenient, and to be justified for the purpose of the present study.

## FORMULATION OF THE MODEL

The Dardanelles Strait is approximated by a rectangular channel of variable width and depth. The horizontal coordinate,  $x$ , is taken along the channel and points towards the Marmara Sea from which the surface layer flow moves into the channel. The vertical coordinate,  $z$ , is directed vertically upwards, the channel bottom being located at  $z = -h(x)$ . The initial positions of the free surface and of the interface are located at  $z = 0$  and  $z = -h_1$ , respectively. Their corresponding displacements, as a response to a developing two-layer exchange flow through the channel, are represented by  $d_1(x, t)$  and  $d_2(x, t)$  (Fig. 4). We invoke the incompressibility, hydrostatic and Boussinesq approximations and incorporate vertical mixing by the two-way entrainment across the interface. Under these approximations and idealizations, the cross-sectionally averaged two-layer form of the equations may be written as (Grubert, Abbott, 1972; Hodgins, 1979; Sur, 1988)

$$b H_{1t} + q_{1x} = b(w_{e1} - w_{e2}) \quad (1)$$

$$b H_{2t} + q_{2x} = b(w_{e2} - w_{e1}) \quad (2)$$

$$q_{1t} + (u_1 q_1)_x = -gb H_1 d_{1x} + b(\tau_s - \tau_i) + b\{u_2 w_{e1} - u_1 w_{e2}\} + L_1(u) \quad (3)$$

$$q_{2t} + (u_2 q_2)_x = -gb H_2 [r d_{1x} + \varepsilon d_{2x}] + b(\tau_i - \tau_b) + b\{u_1 w_{e2} - u_2 w_{e1}\} + L_2(u) \quad (4)$$

Here subscripts 1 and 2 refer to the upper and lower layers, respectively;  $b(x)$  denotes the width of the channel;  $u_k$  is the longitudinal velocity;  $H_k$  is the thickness;  $q_k = b H_k u_k$  is the volume flow rate;  $\rho_k$  is the density of the layer  $k$  ( $k = 1, 2$ );  $\rho_0$  is a water density representative of the entire water column;  $r = \rho_1/\rho_2$ ;  $\varepsilon = (1-r)$ ;  $g$  is the gravitational acceleration; and  $g' = g\varepsilon$  is the reduced gravity;  $\tau_s$ ,  $\tau_b$  and  $\tau_i$  are the boundary shear stresses (divided by  $\rho_0$ ) at the surface, bottom and at each side of the interface, respectively;  $L_k(u)$  signifies an operator simulating the horizontal mixing of momentum due to the turbulent scale processes in each layer;  $w_{e1}$ ,  $w_{e2}$  represent the entrainment velocities in the upward and downward directions, respectively. Subscripts  $t$  and  $x$  denote the partial differentiations with respect to time and the horizontal coordinate, respectively.

Instantaneous local thicknesses of the layers are defined by

$$H_1 = h_1 + d_1 - d_2, \quad H_2 = h_2 + d_2 \quad (5)$$

Shear stresses at the boundaries are expressed by (Pedersen, 1980)

$$\tau_s = (\rho_s/\rho_0) c_s |W| W \quad (6)$$

$$\tau_b = c_b |u_2| u_2 \quad (7)$$

$$\tau_i = c_i |u_1 - u_2| (u_1 - u_2) \quad (8)$$

where  $\rho_a$  is the density of air,  $W$  is the mean wind speed at 10 m above the sea surface, and  $c_s$ ,  $c_b$ ,  $c_i$  are the dimensionless drag coefficients. The horizontal mixing term,  $L_k(u)$ , is approximated by

$$L_k(u) = [N_k q_{kx}]_x \quad (k = 1, 2) \quad (9)$$

where the horizontal eddy coefficient,  $N_k$ , is expressed following Stacey and Zedler (1986) as

$$N_k = \alpha \Delta x^2 |u_{kx}| \quad (k = 1, 2) \quad (10)$$

with  $\alpha$  representing a constant parameter chosen arbitrarily and  $\Delta x$  being the horizontal grid increment. ( $\alpha^{1/2} \Delta x$ ) is, therefore, made proportional to the hori-

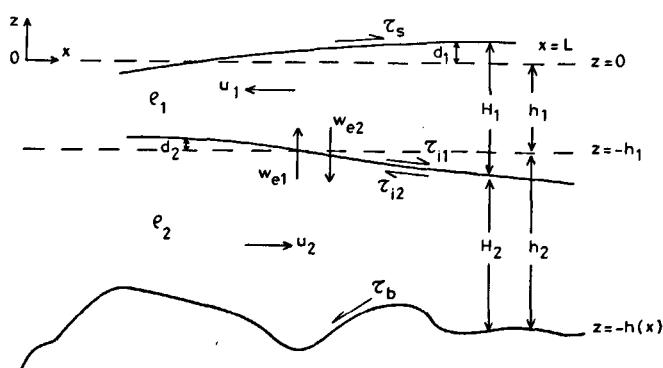


Figure 4  
Definition sketch for some model parameters.

zontal mixing length scale in (10). Our principal concern in incorporating the horizontal mixing term in the model is to smooth out any developing discontinuity associated with the formation of an anticipated internal hydraulic jump.

For the two-layer flows, the hydraulic condition is simply determined by the value of the composite Froude number  $G^2$  (Armi, 1986):

$$G^2 = F_1^2 + F_2^2 \quad (11)$$

where  $F_k^2 = u_k^2/g' H_k$  ( $k=1, 2$ ) is the densimetric Froude number for each layer expressing the ratio of kinetic to potential energy of the flow. Hydraulic control occurs when the flow is critical, corresponding to the condition  $G^2=1$ . A control point separates subcritical flow ( $G^2 < 1$ ) from supercritical flow ( $G^2 > 1$ ).  $G^2$  is also interpreted as the parameter characterizing the degree of nonlinearity of the flow.

The two-way entrainment process is parameterized by means of the constant flux Richardson number,  $R_f$ , concept as (e.g. Çeçen *et al.*, 1981; Pedersen, 1980; Stigebrandt, 1981; Moller, Pedersen, 1983)

$$1/2 g' H_k w_{ek} = R_f PRD_k \quad (k=1, 2) \quad (12)$$

where the form of  $PRD_k$  representing the rate of turbulent energy production is given for each layer by (Sur, 1988)

$$PRD_1 = [\gamma W \tau_s + 1/2(u_1 - u_2) \tau_i + 1/2(u_1 - u_2)^2 w_{e1}] \quad (13a)$$

$$PRD_2 = [\beta u_2 \tau_b + 1/2(u_1 - u_2) \tau_i + 1/2(u_1 - u_2)^2 w_{e2}] \quad (13b)$$

In (13 a, b),  $\gamma$  and  $\beta$  are disposable constant parameters;  $\gamma W$  represents the surface drift velocity which is related linearly to the wind speed (Kullenberg, 1982). The first two terms express the turbulent energy productions associated with the work done by the boundary stresses. The final terms are related with the losses of mean flow kinetic energy in the layers due to the velocity shear at the interface and consequently the gain in the turbulent energy to be utilized in the entrainment process.

Equation (12) expresses the efficiency of the entrainment process such that the net rate of turbulent kinetic energy available for the entrainment process in the layer is used to increase its level of potential energy by entrainment. Pedersen (1980) notes that application of (12) to supercritical flows may not be completely adequate because it considers only the gain in the potential energy, while it neglects the gain in the turbulent kinetic energy itself associated with the entrainment process. Incorporation of the latter contribution in the entrainment parameterization, however, requires parameterization of turbulent kinetic energies in terms of the mean currents by introducing an empirical parameter representing a measure of the degree of turbulence. This has been avoided here, in order not to introduce an extra empiricism into the model. For subcritical flows, Kullenberg (1977) found the range of values for  $R_f$  as  $0.07 \leq R_f \leq 0.13$ . Compiling and analysing all the relevant experimental data reported

to date, Pedersen (1980) notes that whereas  $R_f$  could be as small as 0.04 for subcritical flows, it may attain a higher value of 0.18 for supercritical flows.

The net entrainment flux across the interface is defined by

$$q_e = (2 \Delta x) b [w_{e1} - w_{e2}] \quad (14)$$

which is positive when directed upwards from the lower to the upper layer.  $2 \Delta x$  is the distance between two successive current points of the staggered grid system.

### Boundary conditions

Boundary conditions describing subcritical flow conditions are specified at the open boundaries. At the southwestern exit section of the Dardanelles the model channel is, therefore, extended partially to the adjacent Aegean Sea by introducing a gradual increase in its width so that the anticipated exit control may be simulated as the flow experiences a sharp transition at the actual Aegean-Dardanelles junction.

Specification of subcritical flow conditions implies application of one boundary condition for each layer at the end points. In the present model, we prescribe the surface and interfacial elevations by making use of the radiation conditions. Accordingly, at the Marmara end of the channel (at  $x=L$ ), the conditions are (Sur, 1988)

$$d_1 = (gh)^{-1/2} [(h_1 u_1 + h_2 u_2) + 2 Q_{1L}/b] \quad (15)$$

$$d_2 = (h_2/h) d_1 - (h_1 h_2/g' h)^{1/2} [(u_1 - u_2) + Q_{2L} h/(b h_1 h_2)]. \quad (16)$$

Similarly, at the Aegean end of the channel (at  $x=0$ ), the conditions are

$$d_1 = -(gh)^{-1/2} [(h_1 u_1 + h_2 u_2) + 2 Q_{10}/b] \quad (17)$$

$$d_2 = (h_2/h) d_1 + (h_1 h_2/g' h)^{1/2} [(u_1 - u_2) + Q_{20} h/(b h_1 h_2)], \quad (18)$$

where  $Q_L$ 's and  $Q_0$ 's are the prescribed volume transports to force the two-layer flow system through the open boundaries. As defined before,  $h_1$  and  $h_2$  represent the equilibrium depths of the upper and lower layers, respectively, and  $h$  denotes the undisturbed depth of the water (*cf.* Fig. 4). In the numerical discretization procedure, these conditions are actually applied at points  $x = \Delta x$  and  $x = L - \Delta x$  corresponding to the current points of the staggered grid system. The values of  $d_1$ ,  $d_2$  at these current points are specified by simple averaging from the adjacent grid points which therefore introduces the  $d_1$ ,  $d_2$  at the boundary.  $u_1$ ,  $u_2$  are specified explicitly in terms of their known values obtained at the previous time-step.

Partial extension of the model domain out into the Aegean Sea also makes the radiation conditions applicable at the southwestern end of the channel. The radiation boundary concept is formally based on the linearized shallow water theory and is consequently valid only for a region where linearization is locally feasible. This may not be the case in the close proximity of the actual Aegean exit, where the flow may strictly be nonlinear due to anticipated controlled flow condition.

RESULTS

The length of the channel being modelled,  $L$ , is taken to be 76 km which allows for partial extension of the actual strait on each side. It is divided into 152 sections of 500 m length at which the smoothed width and depth variations are specified from navigation charts. The actual points of communication of the strait with the Aegean and Marmara Seas are located at grid points 12 and 142, respectively. The Marmara end of the strait corresponds to the Gelibolu-Çardak section located near station C3 (cf. Fig. 1 b). Abrupt expansion of the strait at the Aegean exit section is approximated by increasing the width artificially to 13 km at a distance of 6 km within the southeastern extremity of the model channel. The Nara contraction coincides with grid points 57 and 58, where the width is taken as 1 250 m. The laterally-averaged estimates of depth are accepted as representative values of  $h(x)$  at the grid points.

The equations governing the exchange flow in the Dardanelles Strait are solved by forward in time and centered in space explicit finite difference methods. The grid is staggered so that the independent variables (layer thicknesses and layer transports) are predicted at consecutive grid points. Their values at the points to which they are not assigned are computed by averaging. Stability of the numerical scheme is secured by taking  $\Delta t = 15$  s. The dynamical equations, starting from an initial state of rest, are integrated forward in time until a final steady-state response is established at all grid points in the channel.

The values of forcing parameters used in (15)-(18) are adjusted in the experiments until the predicted values of flow rates at the actual boundaries (i.e., at grid points 12 and 142) become consistent with their long term estimates deduced from the two-layer water and salt budget calculations (Özsoy *et al.*, 1986). Some experimentation was necessary before this purpose could be achieved. The experiment we describe here corresponds to a parametric setting given in the Table, and concerns the two-way exchange flow established in the strait in response to the inflow forcings prescribed at the boundaries.

Variations of the interface position, the currents in the layers, the composite Froude number and the net

Table

Values of parameters used in the model.

$c_f = 0.0012$	$c_b = 0.0013$
$g = 9.81 \text{ m/s}^2$	$g' = 0.086 \text{ m/s}^2$
$\alpha = 5$	$\beta = 1/3$
$Rf = 0.13$	$\gamma = 0.02$
$\lambda = 1.5 \cdot 10^{-6}$	$W = 0 \text{ m/s}$
$L = 76 \text{ km}$	$h_i = 22 \text{ m}$
$\Delta x = 500 \text{ m}$	$\Delta t = 15 \text{ s}$
$M = 153$	$\rho_0 = 1\,000 \text{ kg/m}^3$
$\rho_1 = 1\,019 \text{ kg/m}^3$	$\rho_2 = 1\,029 \text{ kg/m}^3$
$Q_{10} = 0$	$Q_{1L} = 40\,000 \text{ m}^3/\text{s}$
$Q_{20} = 120\,000 \text{ m}^3/\text{s}$	$Q_{2L} = 60\,000 \text{ m}^3/\text{s}$

entrainment flux across the interface are shown in Figure 5. When the steady state is achieved, the upper- and lower-layer flows entering into the channel from its Marmara and Aegean ends are respectively about  $28053 \text{ m}^3/\text{s}$  and  $24962 \text{ m}^3/\text{s}$ . The net interfacial transport taking place between the Marmara end and grid point 60 (1 km upstream of the Nara contraction) is in the downward direction and amounts to about  $335 \text{ m}^3/\text{s}$ , accounting for approximately 1% of the Marmara inflow. This part of the channel is characterized by weak subcritical flows in both layers, the composite Froude number being less than 0.1. The position of the interface, which is initially set to 22 m below the free surface, is tilted linearly upwards from a depth of 31 m at the Marmara end of the channel to 23 m at grid point 60. The currents in both layers attain values of 25 cm/s on average. As the upper-layer flow proceeds towards the Aegean end of the channel, significant changes are observed in its structure. The surface flow, which attains a value of  $27\,718 \text{ m}^3/\text{s}$  just upstream of the Nara Pass, increases to  $30\,504 \text{ m}^3/\text{s}$  at grid point 12 and then eventually reaches  $33\,394 \text{ m}^3/\text{s}$  at the southwestern extremity of the channel. The region downstream of the Nara Pass is, therefore, characterized by about  $5\,676 \text{ m}^3/\text{s}$  excess in the amount of the surface flow, accounting approximately for 23% of the Aegean inflow.

As the upper layer flow passes through the Nara contraction, the composite Froude number,  $G^2$ , exceeds unity, implying transition of the flow to supercritical state with the control point occurring at the narrowest section located at grid point 58. Immediately downstream of the Nara Pass, the interface depth rises

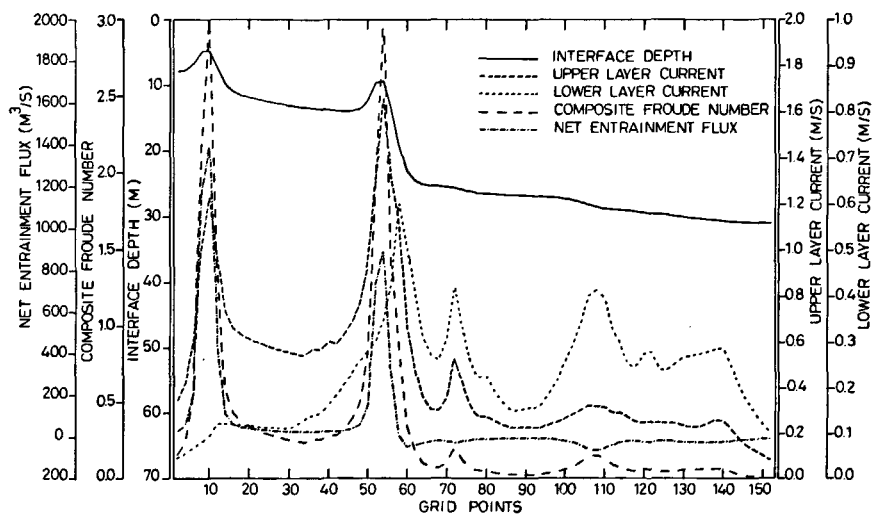


Figure 5  
Model predictions of variations of the interface depth, the upper- and lower-layer currents, the composite Froude number and the net entrainment flux along the Dardanelles.

abruptly towards the free surface. It attains its shallowest position with approximately 9.6 m below the free surface at 2 km downstream of the narrowest section. The currents in both layers tend to accelerate, yielding the strongest upper layer current ( $\approx 165$  cm/s) and the corresponding maximal value of  $G^2$  ( $\approx 3.0$ ). Further southwestward, the upper-layer current begins to decelerate with a corresponding deepening of the interface depth. At grid point 50, the upper-layer current and the interface depth attain values of about 93 cm/s and 12.5 m. The value of  $G^2$  is 0.8, implying transition of the flow to subcritical state by undergoing an internal hydraulic jump. Further downstream of grid point 50, currents in the upper layer continue decelerating and the net upward interfacial transport diminishes significantly. The interface declines further and reaches 14.2 m at grid point 44, after which the interface depth tilts linearly upwards as in the north-eastern reaches of the channel.

Features similar to those observed in the vicinity of the Nara Pass are repeated in the Aegean-Dardanelles junction region. As the upper layer flow exits from the abruptly widening junction section, the flow again passes through the critical state at grid point 12. The upper-layer current increases to a value of 125 cm/s at grid point 10, coinciding with a minimal interface depth of approximately 5.0 m, and with maximal value of the composite Froude number of 3.32. Thereafter, the upper-layer flow re-establishes its subcritical state at grid point 6 by undergoing another internal hydraulic jump as it eventually joins the Aegean basin.

The regions extending horizontally 3-5 km downstream of the Nara contraction and the Aegean exit of the Dardanelles are, therefore, characterized by relatively strong upper-layer currents (generally exceeding 100 cm/s), significant nonlinear variations in the position of the interface depth, and intense net upward interfacial transport. These features seem to compare favorably with the observations (*cf.* Fig. 2 and 3).

An important aspect of the water exchange through the Dardanelles Strait is the influence of the internal hydraulics on the exchange process, *i.e.* the question whether or not the exchange is maximal and thus

actually limited by the controls. As discussed by Farmer and Armi (1986), if the exchange is hydraulically controlled at both ends of a channel, the supercritical flows on either side of the control sections effectively isolate the two-way exchange from the adjacent reservoir conditions. In this case, the exchange is referred to as maximal and is fully determined by the conditions within the channel and not dictated by the conditions in the reservoirs. However, submaximal exchanges may also be possible when one of the exit controls is lost and flow becomes critical at one end of the channel only. In this case, the reservoir conditions contribute to the exchange along the channel, and the flow is no longer fully determined by the conditions within the channel. For typical observed flow conditions through the Dardanelles, the numerical experiments indicate presence of submaximal exchange along the strait since the lower-layer flow is not subject to an internal hydraulic control at its Marmara exit. The lower-layer flow meets the Marmara Sea through a gradually widening junction region with a relatively large cross-sectional area which, together with additional contribution of the bottom friction, gives rise to currents which are not sufficiently strong to impose a critical control. In reality, the necessary condition constraining the lower-layer flow takes place further east, at the northern sill of the Bosphorus Strait (Özsoy *et al.*, 1986).

Dynamics of the two-layer exchange flow in the Dardanelles may further be examined by analyzing the upper layer momentum balance. As shown in Figure 6, the horizontal momentum diffusion and the interfacial momentum transfer due to the entrainment process appear to have negligible effects throughout the channel, and a weak balance of terms generally exists in its subcritical regions. Notable changes, however, take place in the horizontal advection and pressure gradient terms near the Nara contraction and the Aegean exit regions. As the upper layer current passes through the Nara control section and accelerates, a steep negative gradient of horizontal momentum flux is established up to grid point 58. This, together with the partial contribution of the interfacial stress, is balanced by a

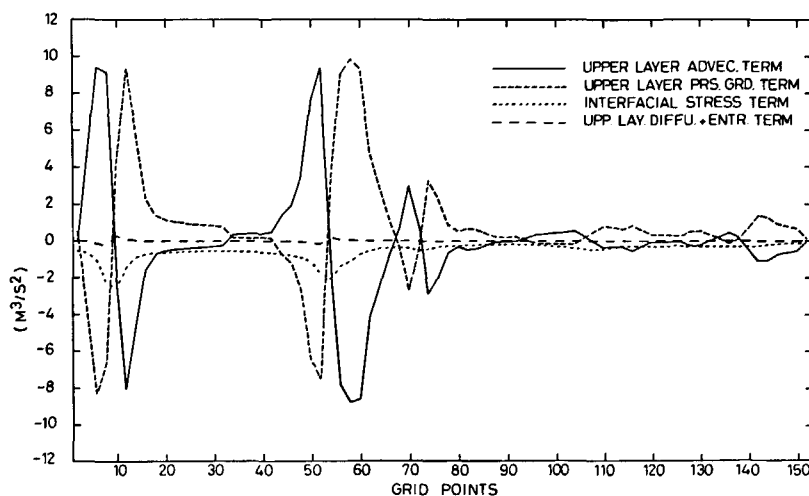
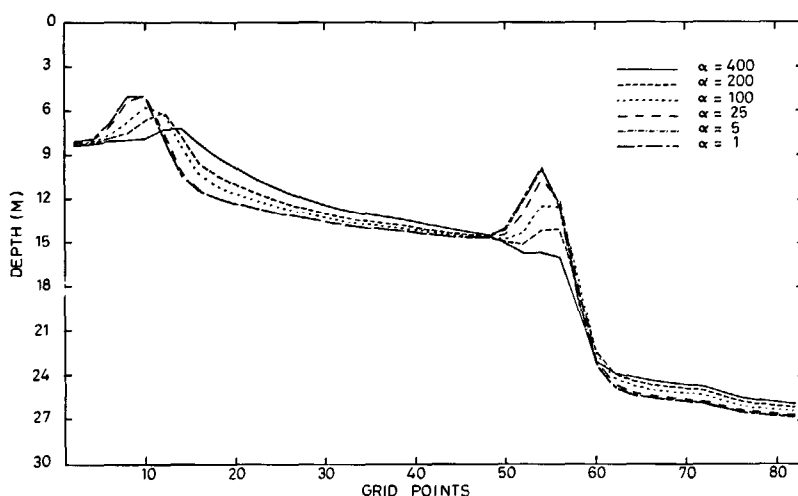


Figure 6  
Model predictions of variations of terms in the upper layer momentum equation.

Figure 7  
Model predictions of variation of interface depth for the various values of  $\alpha$ .



strong positive horizontal pressure gradient. As the upper layer current continues to accelerate at a decreasing rate downstream of the Nara control section, the magnitudes of the horizontal advection and the horizontal pressure gradient terms decrease. This reduction continues up to grid point 54, where they almost vanish. This point, in fact, corresponds to the shallowest position of the interface and the strongest upper-layer current. In the decelerating phase of the surface layer current, balance between the horizontal pressure gradient and the horizontal advection is reversed, leading to the deepening of the interface depth. Though this feature continues further southwest, the deepening is most pronounced up to grid point 50, at which the flow returns to its subcritical state. Thereafter, a weak balance of terms is again observed, with the negative contribution of the horizontal advection balanced by the positive pressure gradient and consequently giving rise to a smooth elevation of the interface. The surface flow reaching the Aegean exit region undergoes similar stages which cause further rising of the interface and its subsequent deepening as the upper-layer flow joins the open ocean.

#### Model dependence on some external parameters

The values of the empirical parameters employed in the experiments are deduced through a series of calibration and sensitivity studies. The criterion adopted for setting the value of  $\alpha$  is to choose its smallest possible value which will be able to provide a stable numerical solution in the vicinity of internal hydraulic jumps. It is found that the two-layer flow structure is unaffected by the choice of the value of  $\alpha$  for less than 10, and even  $\alpha \rightarrow 0$  leads to numerically stable results. Higher values of  $\alpha$ , on the other hand, result in smoother fields of the currents and interface depths since a relatively higher rate of dissipation is introduced into the model. Variations of the interface depth in the lower half of the strait are shown for various values of  $\alpha$  in Figure 7. For the value of  $c_i$  between 0.00125 to 0.0025, corresponding to a range reported in the literature (*cf.* Pedersen, 1980), the flow dynamics appears not to be sensitive to the value of the bottom drag coefficient. Only the lower layer currents have been affected slightly, whereas the features associated with the

hydraulic controls and downstream adjustment of the supercritical surface layer flow were almost identical. The interface depth and the magnitudes of the currents in the layers, as well as the net rate of interfacial transport are, however, found to be sensitively dependent upon the value of interfacial drag coefficient (Fig. 8a-e). As the value of  $c_i$  is increased from 0.0012 to 0.0028, because of the higher rate of dissipation introduced into the model, the strength of currents in the layers decreases (Fig. 8b). Consequently, the net interfacial transport between the layers decreases (Fig. 8a), and the development of controlled flow conditions and associated internal hydraulic jumps diminish. For  $c_i = 0.0028$ , the Nara contraction becomes no longer a control section and the surface flow attains its subcritical state throughout the channel up to the Aegean exit section (Fig. 8d). Development of hydraulically controlled flow at the Nara contraction then calls for much higher inflow rates at the boundaries which, however, lead to unreasonably small currents in the lower layer although an effort is made to increase the lower-layer flow as much as possible. This feature of the model, therefore, implies that the value of the interfacial friction coefficient is crucially important for simulating the flow structure consistent with the observations. It turns out that the interfacial drag coefficient used in (8) should be smaller than 0.0020 for the case of the Dardanelles Strait. This is in agreement with the experimental findings reported in Pedersen (1980).

#### SUMMARY AND CONCLUSIONS

Water exchange through the Dardanelles Strait is studied by a two-layer model which approximates the laterally averaged flow by two homogeneous layers of differing density separated by an entraining interface. Principal emphasis is given to possible explanation of the observed asymmetry and rapid transition of the interface depth in terms of the hydraulic characteristics of the flow.

For typical rates of inflow from the Marmara and Aegean Seas, it is shown that the strait possesses a submaximal exchange. As the lower layer flows subcritically through the strait without undergoing an internal hydraulic control, the upper-layer flow is controlled

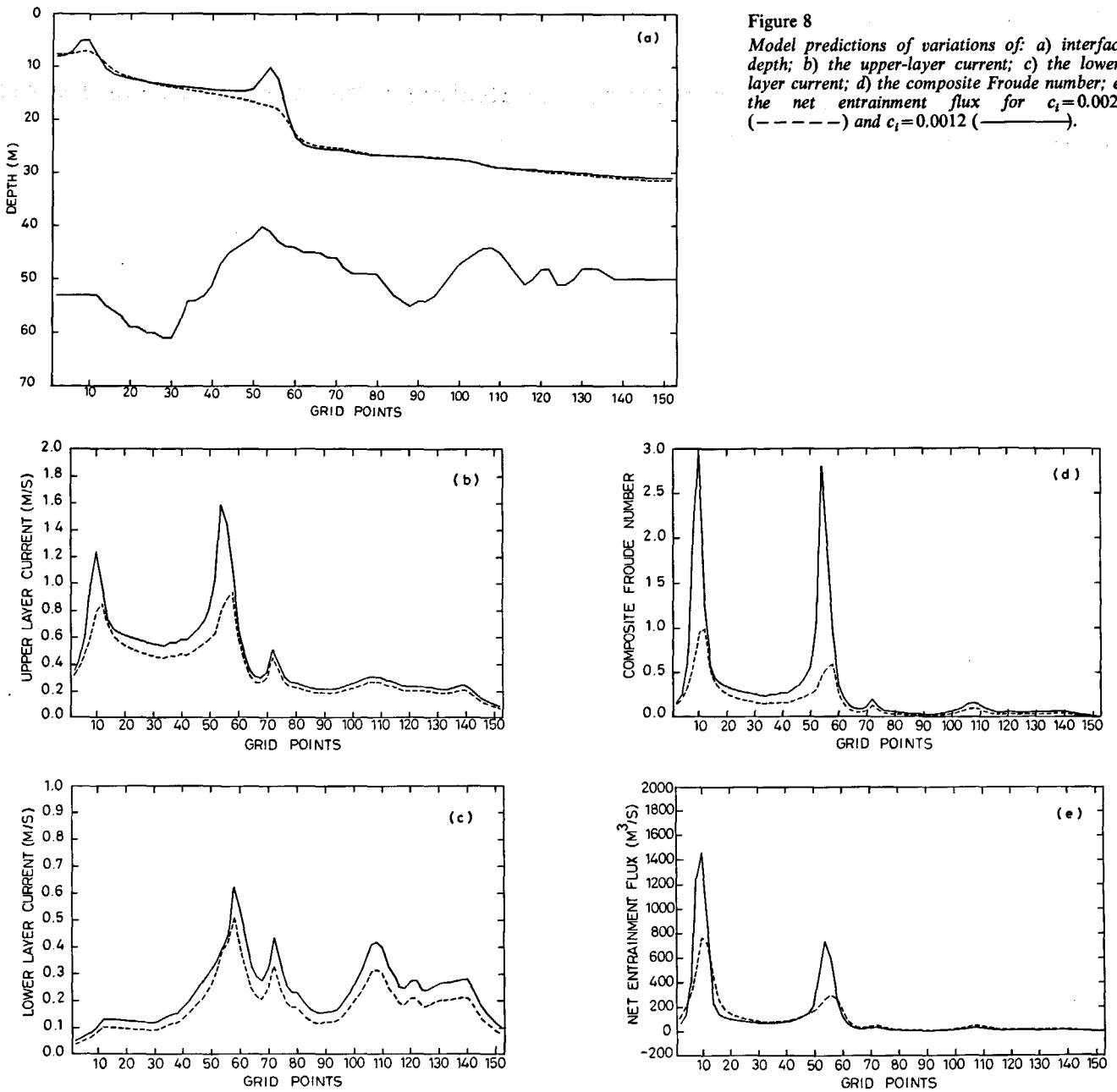


Figure 8  
 Model predictions of variations of: a) interface depth; b) the upper-layer current; c) the lower-layer current; d) the composite Froude number; e) the net entrainment flux for  $c_i=0.0028$  (-----) and  $c_i=0.0012$  (—————).

due to contraction at Nara Pass and abrupt expansion at the Aegean end. The upper layer Marmara inflow, which is subcritical at the northeastern part of the strait, reaches the critical state at the Nara contraction and then becomes supercritical with increased currents in the shallower interface depth downstream of the narrowest section. Further southwest, as the interface deepens, the upper layer flow adjusts itself to the subcritical state by undergoing an internal hydraulic jump. This is repeated at the Aegean termination of the strait. The upper-layer flow is subject to the critical transition at the abruptly widening Aegean exit, and eventually joins the Aegean basin in its subcritical state after undergoing another internal hydraulic jump just outside the Aegean-Dardanelles junction.

For the particular inflow rates used in deriving the two-layer transport in the strait, the model predicts 23% of the Aegean influx to be transported into the upper layer by the entrainment process and restored to the sea of origin. In accord with the regions of increased current shear at the interface and the shallower inter-

face depth, the regions of supercritical upper layer flow downstream of the control sections are identified as being two particular regions of intense mixing.

The flow structure established in the Dardanelles appears to be particularly sensitive to the value of the interfacial friction coefficient. It emerges that the currents in the layers weaken considerably and that the internal hydraulic controls are lost for the value of  $c_i$  less than 0.0020. An important implication of this is the significant reduction in the net upward interfacial transport which normally takes place in the regions of supercritical flow downstream of the control sections. Furthermore, the value of  $\alpha$  used in the parameterization of the turbulent exchange coefficients should be chosen as small as possible being able to provide the stable numerical solutions in the vicinity of internal hydraulic jumps. As a result of introducing more horizontal dissipation into the model, higher values lead to development of weaker flow fields and reduce the nonlinearity of the flow which is the essential aspect of the internally controlled flows.



## Acknowledgements

We are indebted to Bryan Johns for his assistance in developing the model. We thank many colleagues, particularly Ü. Ünlüata, I. Ünsal, E. Özsoy and M. A.

Latif, as well as the referees, for discussion and their helpful comments. We are grateful to M. Ünsal for preparing the French version of the Abstract.

## REFERENCES

- Armi L., 1986. The hydraulics of two flowing layers with different densities, *J. Fluid Mech.*, **163**, 27-58.
- Armi L., Farmer D. M., 1985. The internal hydraulic of the Strait of Gibraltar and associated sills and narrows, *Oceanol. Acta*, **8**, 1, 37-46.
- Armi L., Farmer D. M., 1986. Maximal two-layer exchange through a contraction with barotropic net flow, *J. Fluid Mech.*, **164**, 27-51.
- Çeçen K., Beyazit M., Sümer M., Güçlüer S., Doğusal M., Yüce H., 1981. Oceanographic and hydraulic investigation of the Bosphorus. vol. 1, Technical report submitted to the Irrigation Unit of the Turkish Scientific and Technical Research Council, Fac. Civil Engineering, Tech. Univ. Istanbul, 166 p (in Turkish).
- Farmer D. M., Armi L., 1986. Maximal two-layer exchange over a sill and through the combination of a sill and contraction with barotropic net flow, *J. Fluid Mech.*, **164**, 53-76.
- Farmer D. M., Denton W. A., 1985. Hydraulic control of flow over the sill in Observatory Inlet, *J. Geophys. Res.*, **90**, 9051-9068.
- Grubert J. P., Abbott M. B., 1972. Numerical computation of stratified nearly horizontal flows, *J. Hydr. Div. ASCE*, HY10, 1847-1863.
- Hodgins H. O., 1979. A time dependent two-layer model of fjord circulation and its application to Albeni Inlet, British Columbia, *Estuarine Coastal Mar. Sci.*, **8**, 361-378.
- Kullenberg G., 1977. Entrainment velocity in natural stratified shear flow, *Estuarine Coastal Mar. Sci.*, **5**, 329-338.
- Kullenberg G., 1982. Physical Process, in: *Pollutant transfer and transport in the sea*, vol. 1, Chap. 1, edited by G. Kullenberg, 1-89, CRC Press.
- Moller J. S., Pedersen F. B., 1983. Internal seiches in a stratified sill fjord, Technical University of Denmark, Institute of Hydrodynamics and Hydraulic Engineering, *Progr. Rep.*, **58**, 31-40.
- Özsoy E., Oğuz T., Latif M. A., Ünlüata Ü., 1986. Oceanography of the Turkish Straits- First Annual Report, vol. 1, Physical Oceanography of Turkish Straits. Technical Report submitted to the Istanbul Water and Sewerage Administration, Inst. Mar. Sci., Middle East Tech. Univ., 108 p.
- Pedersen F. B., 1980. A monograph on turbulent entrainment and friction in two-layer stratified flow, Inst. Hydrodynamics and Hydraulic Engineering, Tech. Univ. Denmark. Ser. Pap., **25**, 397 p.
- Stacey M. W., Zedel L. J., 1986. The time-dependent hydraulic flow and dissipation over the sill of Observatory Inlet, *J. Phys. Oceanogr.*, **16**, 1062-1076.
- Stigebrandt A., 1981. A mechanism governing the estuarine circulation in deep, strongly stratified fjords, *Estuarine, Coastal. Shelf Sci.*, **13**, 197-211.
- Sur H. I., 1988. Numerical modelling studies of two-layer flows in the Dardanelles Strait and the Bay of Izmit, *Ph. D. Thesis, Inst. Mar. Sci., Middle East Tech. Univ.*, 245 p.
- Wang D. P., 1987. Strait surface outflow, *J. Geophys. Res.*, **92**, 10807-10825.